Annals of Botany **117**: 643–651, 2016
doi:10.1093/aob/mcw004, available online at www.aob.oxfordjournals.org

ANNALS OF BOTANY
Founded 1887

The expression of light-related leaf functional traits depends on the location of individual leaves within the crown of isolated *Olea europaea* trees

Adrián G. Escribano-Rocafort[1,*], Agustina B. Ventre-Lespiaucq[1], Carlos Granado-Yela[2], Rafael Rubio de Casas[3,4,5], Juan A. Delgado[1] and Luis Balaguer[2,§]

[1]Department of Ecology, Faculty of Biology, Complutense University of Madrid, Jose Antonio Novais St., 28040 Madrid, Spain, [2]Department of Plant Biology I, Faculty of Biology, Complutense University of Madrid, Jose Antonio Novais St., 28040 Madrid, Spain, [3]Department of Ecology, Facultad de Ciencias, Universidad de Granada, Avda. de la Fuentenueva s/n, 18071 Granada, Spain, [4]Estación Experimental de Zonas Áridas, EEZA-CSIC, Carretera de Sacramento s/n, Almería, Spain and [5]UMR 5175 CEFE - Centre d'Ecologie Fonctionnelle et Evolutive (CNRS), 1919 Route de Mende, F-34293 Montpellier cedex 05, France
** For correspondence. E-mail adrianescribano@ucm.es*
[§]Deceased.

Received: 2 October 2015 Returned for revision: 7 November 2015 Accepted: 27 November 2015 Published electronically: 4 March 2016

• **Background** The spatial arrangement and expression of foliar syndromes within tree crowns can reflect the coupling between crown form and function in a given environment. Isolated trees subjected to high irradiance and concomitant stress may adjust leaf phenotypes to cope with environmental gradients that are heterogeneous in space and time within the tree crown. The distinct expression of leaf phenotypes among crown positions could lead to complementary patterns in light interception at the crown scale.
• **Methods** We quantified eight light-related leaf traits across 12 crown positions of ten isolated *Olea europaea* trees in the field. Specifically, we investigated whether the phenotypic expression of foliar traits differed among crown sectors and layers and five periods of the day from sunrise to sunset. We investigated the consequences in terms of the exposed area of the leaves at the tree scale during a single day.
• **Key Results** All traits differed among crown positions except the length-to-width ratio of the leaves. We found a strong complementarity in the patterns of the potential exposed area of the leaves among day periods as a result of a non-random distribution of leaf angles across the crown. Leaf exposure at the outer layer was below 60 % of the displayed surface, reaching maximum interception during morning periods. Daily interception increased towards the inner layer, achieving consecutive maximization from east to west positions within the crown, matching the sun's trajectory.
• **Conclusions** The expression of leaf traits within isolated trees of *O. europaea* varies continuously through the crown in a gradient of leaf morphotypes and leaf angles depending on the exposure and location of individual leaves. The distribution of light-related traits within the crown and the complementarity in the potential exposure patterns of the leaves during the day challenges the assumption of low trait variability within individuals.

Key words: Crown structure, leaf traits, leaf exposure, direct light, *Olea europaea*, isolated trees, high irradiance, leaf angles, daily pattern, variation within individuals.

INTRODUCTION

Trees are able to adjust foliar trait phenotype in response to the environment and within-crown gradients. The spatial heterogeneity across the tree crown could promote the expression of phenotypic differences in foliar traits and the prevalence of a set of coordinated traits (individual's phenotypic syndrome). The phenotypic syndrome meets the limitations of the experienced environment that affect the fitness of the whole plant (Jurik *et al*., 1979; Howell *et al*., 2002; Falster and Westoby, 2003; Pearcy *et al*., 2005; Marks and Lechowicz, 2006; Valladares and Niinemets, 2008; Wilson and Nussey, 2010). The variability in leaf traits within the tree crown is functionally relevant. The plasticity in structural traits such as leaf angle and size can have profound consequences for the acquisition of the light resource (Howell *et al*., 2002; Falster and Westoby, 2003). Indeed, plasticity of leaf inclination angles alters light properties within the tree crown, enhancing whole-individual carbon gain (Uemura *et al*., 2006). Modifying light transmission and light properties can confer on trees advantages such as a higher degree of control of photosynthesis, transpiration and energy balance (Pearcy and Yang, 1996). Considering the modular nature of plants, the phenotypic response of the whole tree could be enhanced by the integrated expression of leaf phenotypes among functional units of the tree crown (de Kroon *et al*., 2005; Granado-Yela *et al*., 2011). The most and least exposed leaves within the tree crown (hereafter referred to as the outer and inner layer, respectively) constitute a classic example of functional subunits that are spatially segregated and specialized in the harvesting of a heterogeneous light resource (Sack *et al*., 2006). Nevertheless, the realized phenotypic diversity will necessarily be constrained by other abiotic and biotic factors. As a

consequence, the expression of leaf attributes related to light interception may be adjusted to the patterns of irradiance and concomitant stress of a local environment.

Intrinsically, tree growth generates local differences in the environment experienced by each portion of the crown. On isolated trees the efficiency of direct light interception is strongly dependent on the environmental conditions and on leaf attributes, which in turn are affected by crown shape and structure (Ackerly and Bazzaz, 1995; Farnsworth and Niklas, 1995; Planchais and Sinoquet, 1998; Farque *et al*., 2001; Falster and Westoby, 2003). Considering the direct component of the light in the sky, the potential light capture achieved by a flat leaf (or any flat surface with defined tilt and orientation angles) during a certain day and at any given latitude is determined by the angle of incidence of the sunbeams to the leaf blade. The mismatch between the sunbeam and the normal vector to the plane of the leaf imposes a reduction in the potential exposed surface due to diurnal changes in the azimuth and altitude of the sun (Granado-Yela *et al*., 2011). However, the estimation of the potential reduction in the exposed leaf surface is trivial once the spatial position of the leaf is defined for a given latitude and time. In high-irradiance environments with other sources of stress, such as high temperatures and low water availability, increases in factors that entail self-shading constitute crucial attributes of plant architecture (Howell *et al*., 2002; Pearcy *et al*., 2005). In fact, minimizing the negative impact of high direct radiation on photosynthesis by means of steep leaf angles appears to compensate for potentially low daily carbon gains in high-irradiance environments (Falster and Westoby, 2003).

The leaf's spatial position (inclination and orientation angles), in addition to the degree of aggregation of leaves, influences the potential of a single leaf to intercept direct sunlight and the penetration of light to lower layers of the crown (Falster and Westoby, 2003). Leaf shape also has an impact on the distribution of light within the crown. Elongated leaf shapes (high length-to-width ratio) can contribute to light-capture efficiency, decreasing self-shading among leaves and enhancing light penetration to deeper layers (Pearcy *et al*., 2005; Sarlikioti *et al*., 2011). Adjustments of leaf traits related to the irradiance experienced by each portion of the crown can lead to spatial specialization and temporal complementarity of productive processes such as carbon fixation, accumulation and carbon export (Granado-Yela *et al*., 2011). Leaf attributes such as low specific leaf area, high leaf length-to-width ratio and high inclination angles at the more exposed layer of the crown can reduce heat loads while having a positive effect on carbon gain at the whole-individual level (Ehleringer and Werk, 1986; Valladares and Pugnaire, 1999; Werner *et al*., 2001, 2002).

Despite the expected within-crown heterogeneity, field designs under natural conditions aimed at characterizing leaf traits and daily patterns of leaf exposure to direct radiation are often restricted to saplings or to extreme positions of the light gradient within the crown (Valladares *et al*., 2005; Gratani *et al*., 2006; Sack *et al*., 2006; Rubio de Casas *et al*., 2007, 2011). However, a higher degree of phenotypic plasticity is expected to occur in reproductive adults under natural conditions across the whole crown (Cavender-Bares *et al*., 2004; Bouvet *et al*., 2005). Therefore, our main aim was to provide a detailed characterization of foliar trait variation across crown positions in order to identify the degree of leaf specialization in a spatio-temporal context and to assess the functional relationship among crown positions. Moreover, estimates of potential leaf exposure at the crown scale are required in individual-based models of vegetation dynamics (e.g. Moorcroft *et al*., 2001; Falster *et al*., 2011). We hypothesized that foliar differentiation would lead to divergent phenotypes and to distinct leaf exposure patterns across the tree crown. To test this hypothesis, we carried out systematic field measurements on a set of functional leaf traits that are related to light interception. Specifically, we characterized leaf angle, area, dry mass and shape (leaf length-to-width ratio) at different crown depths within the crown of ten *Olea europaea* trees growing in two populations with contrasting climates but similar radiation levels. In particular, we investigated whether functional leaf traits were complementary among crown positions. Indeed, variability in leaf angles among crown positions for a given location describe the geometrical relationship between leaf position and the angle of incidence of the incoming radiation, and thus sets the upper limit of potential exposure to direct radiation when self-shading is ignored. Moreover, combined with the investment in area per unit dry mass it can give insight to identify complementary strategies that supposedly optimize light capture from the leaf to the whole-crown level (Granado-Yela *et al*., 2011).

MATERIALS AND METHODS

Species and study site

We studied reproductive individuals of *Olea europaea* ssp. *europaea* (wild olive tree), an evergreen, sclerophyllous, long-lived tree distributed throughout the Mediterranean Basin. This species develops flat leaves that do not track sun movements and was found to have signs of foliar differentiation between the extremes of the light gradient within the tree crown (Granado-Yela *et al*., 2011; Rubio de Casas *et al*., 2011). The present study was conducted in two natural populations located on a Mediterranean island (San Luis [SL], Menorca, Spain) and in the central Iberian Peninsula (Aldea del Fresno [AF], Madrid, Spain). The two populations occurred at equivalent latitudes, thus experiencing similar daylength and sun elevation angles (Table 1). In each population, we selected five individuals that had previously borne fruits with the aim of sampling reproductive adults. Sampling was carried out on isolated trees during one midsummer day in each population (July to August, 2011) to ensure the complete development of leaves, as recommended for woody species under most of the Mediterranean climates in the northern hemisphere (Garnier *et al*., 2001). However, the AF population was located on sloping terrain (~30°, south aspect) and direct sun irradiance decreased on the surrounding terrain during the final hours of daylight. For each population, photosynthetically active radiation (PAR) was extrapolated from the web portal supported by the NASA LaRC POWER Project. Tree canopy structure was comparable across individuals and populations in spite of small differences in the light environment between populations (Table 1). Trees in the SL population were slightly taller than trees in the AF population (Table 1).

TABLE 1. *Studied populations, radiation and tree dimensions per population (mean ± 1 s.e.)*

Location	Coordinates	Altitude (m a.s.l.)	Annual mean direct radiation (μmol m^{-2} s^{-1})[a]	Plant height[b] (m)	Short diameter[b] (m)	Long diameter[b] (m)	Inner layer[b] (m)	Middle layer[b] (m)
Aldea del Fresno, Madrid, Spain	40°19′ N, 4°14′ W	690	923·57 ± 90·15	2·90 ± 0·13	3·31 ± 0·36	3·65 ± 0·49	1·36 ± 0·12	1·08 ± 0·09
San Luis, Menorca, Spain	39°49′ N, 4°16′ E	91	1038·49 ± 97·32	3·30 ± 0·18	4·23 ± 0·36	4·66 ± 0·25	1·30 ± 0·06	0·83 ± 0·05

[a]Monthly averaged midday insolation incident on a horizontal surface. These data were obtained from the NASA Langley Research Center Atmospheric Science Data Center surface meteorological and solar energy (SSE) web portal supported by the NASA LaRC POWER Project.
[b]$n = 5$.

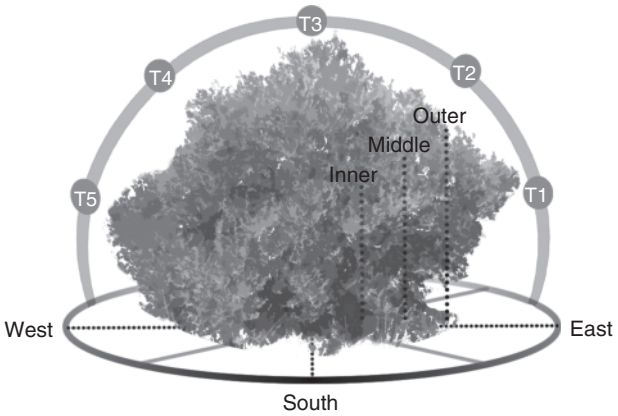

FIG. 1. Sampling design of the tree crown. Representation of sampling points across crown layers and crown sectors. Sampling of outer, middle and inner layers was carried out in the N, E, S and W sectors. Each sector spanned 90°, leaving the main cardinal point in the bisector angle of the crown sector. We sampled 140 leaves per crown. The grey line depicts the sun's trajectory during the chosen day periods (T1–T5) for the instantaneous SAL_t and $STAR_t$ simulations.

Sampling design

Each individual canopy was assimilated to an ellipsoid defined by the maximum diameter of the canopy and its longest perpendicular diameter. Sampling was conducted along the north–south and east–west diameters of the upper half of the ellipsoid, excluding the lower parts of the crown to avoid both self-shading and the effect of cattle grazing (i.e. only the upper semi-ellipsoid was considered). Each sampling axis ('sector' hereafter) was labelled according to its cardinal direction (N, E, S and W) and subdivided into three layers: the outermost layer of leaves, the middle layer of leaves and the deepest layer where leaves were present (Fig. 1). Sampling points for the middle and inner layers were set in an oblique direction from the outer part of the crown towards its geometrical centre. We used a ladder to reach sampling points to avoid crown disturbance. The distance between sampling points along each sector (from the outer to the inner layer) was measured to ensure that all sampling points were comparable and that trees had similar crown depths (Table 1). To account for the decrease in leaf density from the outer to the inner layer, we sampled 20, 10 and 5 leaves in the outer, middle and inner layers of each sector, respectively ($n = 35$ leaves per sector). Only fully expanded leaves were measured. The total number of sampled leaves was 1400 (10 trees × 4 sectors × 35 leaves).

Leaf traits

The relative position of leaves was obtained by measuring *in situ* three leaf angles using an application for smartphones (Nokia N86, Nokia, Spoo, Finland) following Escribano-Rocafort *et al.* (2014). By placing the phone parallel to the desired leaf, leaf elevation angle, midrib-roll angle and leaf azimuth can be easily recorded and stored. The elevation angle of the leaf's midrib was combined with the roll angle around the leaf's midrib and transformed to estimate a leaf's surface inclination angle to the horizontal plane (leaf tilt, L_{tilt}; 0° horizontal, 90° vertical) [eqn (1) in Escribano-Rocafort *et al.*, 2014]. The third measured angle was the orientation of the leaf lamina to true north, i.e. the projection of a normal vector to the leaf's adaxial surface (leaf azimuth, L_{azi}; 0° N, 90° E, 180° S, 270° W). The values of L_{tilt} and L_{azi} were used to estimate the absolute and relative areas intercepting light (see section Potential exposure of the surface of the leaves, below). Measurements were carried out in the absence of wind.

After characterizing the leaf's spatial position, we measured six light-related functional traits on the same leaves to define leaf shape and leaf structure across crown positions. We scanned all collected leaves using a scanner (HP-ScanJet 3800; Hewlett Packard, Palo Alto, CA, USA) to estimate the area of one side of the leaf blade (L_{area}, cm^2), leaf width (L_{width}, cm) and leaf length (L_{length}, cm) using ImageJ (NIH, Bethesda, MD, USA). Leaves were then oven-dried at 65 °C for 48 h and weighed to calculate leaf dry mass (LDM, g) with a precision balance (Mettler Toledo, Greifensee, Switzerland). From these measurements we calculated the two remaining traits: specific leaf area (SLA; leaf area divided by LDM) and leaf shape (L_{index} = leaf length-to-width ratio). To account for allometric differences between individuals, plant size (biovolume) was estimated as:

$$\text{biovolume} = (2/3)\pi(D/2)(d/2)h$$

where D and d are the diameters used to define the canopy ellipsoid and h is plant height. We used biovolume as a size proxy because the total aerial size of wild olives can be approximated with a semi-ellipsoid (Rubio de Casas *et al.*, 2011). Due to missing data, the lowest n considered was 1219 for L_{width}, L_{length} and L_{index}.

Potential exposure of the surface of the leaves

To examine the potential ability of each leaf to capture light, we calculated the silhouette area of the leaf blade (SAL = projection of the leaf blade × leaf area; cm^2) as a

TABLE 2. *Summary statistics for the best linear mixed model fitted to leaf traits and integrated SAL_d and $STAR_d$ across the tree crown with the fixed effects of crown sector, crown layer and the interaction between them*

	numDF	L_{azi} (°)	L_{tilt} (°)	L_{area} (cm^2)	LDM (g)	L_{width} (cm)	L_{length} (cm)	SLA ($cm^2\ g^{-1}$)	L_{index}	SAL_d (cm^2)	$STAR_d$
Sector	3	23·15***	2·49	0·89	3·40*	2·71*	2·05	13·51***	8·19***	–	–
Layer	2	6·49**	29·81***	1·16	38·14***	32·07***	15·80***	233·86***	80·04***	23·38***	26·17***
Sector × layer	6	10·93***	4·46***	3·56**	2·97**	2·84**	2·98**	4·28***	1·44	–	–

numDF, numerator degrees of freedom.
Biovolume was included in all models as a random factor.
The standard deviation of the random components of each model and further details are provided in Supplementary Data Tables S1–S10.
*$P < 0·05$; **$P < 0·01$; ***$P < 0·001$; underscored values are marginally non-significant ($0·05 < P < 0·1$).

measure of leaf area intercepting light, and the silhouette-to-leaf area ratio (STAR = projected area/leaf area), which relates the relative area of the leaf to the angle of incidence of the incoming radiation (Carter and Smith, 1985; Oker-Blom and Smolander, 1988; but see Granado-Yela *et al*., 2011). Both variables combine the trajectory of the sun and the spatial position of an isolated leaf without considering leaf overlapping. Nonetheless, they define the maximum potential area and proportion of the leaf displayed to capture light at a given time due to the angle of incidence of the incoming radiation to a normal vector of the leaf surface (STAR = 1, orthogonal incidence and full potential exposure). Comparisons between SAL and STAR values estimated over the period of 1 day further define when the potential maximum is achieved during the day. To account for light interception variance during the day period we calculated SAL and STAR among crown positions in five evenly distributed periods (SAL_t and $STAR_t$) and as the integral of each leaf over time (from sunrise to sunset) on the day of the measurements (SAL_d and $STAR_d$). To assess SAL_d and $STAR_d$, we calculated the integral of the leaf projection from sunrise to sunset for each leaf among crown positions. Calculations considered leaf angles (L_{azi}, corrected for magnetic declination at each population), location (geographic coordinates) and the sun's position for a given time [eqn (3) in Escribano-Rocafort *et al*., 2014]. We integrated this equation over time for one of the measurement days (31 July), every 2 min. The equation used is sensitive enough to determine whether the exposure occurs in the adaxial or abaxial surface of the leaf (indicated by positive and negative signs, respectively). To assess the variation within the day period, SAL and STAR were calculated for five evenly distributed periods during the day (SAL_t, $STAR_t$; T1–T5, in which T3 equals solar noon) to account for representative sun elevation and azimuth angles in distinct day periods (Fig. 1).

Statistical analyses

We investigated differences in SAL_d, $STAR_d$, SAL_t, $STAR_t$ and leaf traits among crown positions and day periods using a linear mixed effects model. All final models were fitted using restricted maximum likelihood using the nlme package in R software (R Development Core Team, 2008). We determined model selection based on Akaike's information criterion (AIC), obtaining the most explanatory model, weighted by the number of estimated parameters, which includes all significant effects. We included in all models the variables biovolume and population as random intercept to account for differences in leaf exposure due to allometry and local conditions (Rubio de Casas *et al*., 2011). The most complex model included crown sector (with four levels: N, E, S and W), crown layer (three levels; outer, middle and inner) and day period as fixed factors. The most complex random term was plant biovolume nested within population. With the aim of assessing differences between and within day periods, we used linear mixed models for SAL_t and $STAR_t$, adding the fixed term day period (ordered factor with five levels: T1–T5). Multiple comparison tests were performed with the multcomp R package (Bretz *et al*., 2004). Leaf angles were transformed to radians and the remaining leaf traits were log-transformed to improve normality in the analyses. Normality and homoscedasticity assumptions were checked graphically in the final models. A detailed summary of all models and frequency histograms of leaf angles for each crown sector and layer is provided in the Supplementary Data Tables S1–S10 and Figure S1.

RESULTS

Crown structure and leaf traits

Leaf traits differed significantly among crown positions except for L_{index}, SAL_d and $STAR_d$ (Table 2). A detailed summary of all models is provided in the Supplementary Data Tables S1–S10. All crown sectors and layers had a mean L_{azi} oriented towards the south-east except for the middle and inner layer of the N and W sectors, which were facing north-east and south-west respectively (Table 3). Leaf tilt angles in the outer and middle layer in the S and W sectors were more vertical than the rest (L_{tilt} ~60°). The inner layer had the lowest L_{tilt} angles (~45°) except in the S sector, where L_{tilt} values were similar to those displayed in the middle layer (Table 3). Frequency histograms for leaf angles for each crown sector and layer are provided in Supplementary Data Figure S1. Despite an effect of the interaction between crown sector and crown layer, L_{area} was similar among layers and sectors, with maximum differences within the W sector ($2·59 \pm 0·05\ cm^2$ in the outer layer compared with $2·92 \pm 0·08\ cm^2$ in the middle layer) (Table 3). Specific leaf area revealed significant differences between layers (Table 3). The outer layer in the N, E and W sectors had the lowest SLA values (~$47\ cm^2\ g^{-1}$) followed by leaves in the outer layer in the S sector ($52·08 \pm 0·86\ cm^2\ g^{-1}$). Leaves in the inner layer had the highest values of SLA. The L_{index} value did not show an interaction between crown sector and layer (Table 2). Leaves in the E and S sectors were more elongated than those in the N sector. The values of L_{index} were higher in the outer layer than in the middle and inner layers (Table 3).

TABLE 3. *Mean values ± 1 s.e. of leaf traits and integrated values of SAL_d and $STAR_d$ for each crown sector and crown layer*

Crown sector	Crown layer	L_{azi} (°)	L_{tilt} (°)	L_{area} (cm^2)	LDM (g)	L_{width} (cm)	L_{length} (cm)	SLA ($cm^2\,g^{-1}$)	L_{index}	SAL_d (cm^2)	$STAR_d$
N	Outer	116·18 ± 25b	61·94 ± 2·84d	2·77 ± 0·06ab	0·061 ± 0·002e	0·88 ± 0·02bc	4·01 ± 0·06bc	46·36 ± 0·64e	4·76 ± 0·11Aa	0·45 ± 0·02C	0·16 ± 0·01C
	Middle	21·1 ± 35·31ab	49·25 ± 4·78ab	2·78 ± 0·09ab	0·051 ± 0·002bcd	0·91 ± 0·02b	3·90 ± 0·08ab	55·65 ± 1·18bc	4·49 ± 0·14Ab	0·47 ± 0·04B	0·17 ± 0·01B
	Inner	23·29 ± 36·78ab	41·72 ± 4·01a	2·55 ± 0·14ab	0·044 ± 0·003a	0·89 ± 0·02ab	3·60 ± 0·14a	61·23 ± 1·71a	4·09 ± 0·16Ac	0·54 ± 0·05A	0·21 ± 0·02A
E	Outer	109·18 ± 27·81ab	60·44 ± 3·65d	2·72 ± 0·05ab	0·058 ± 0·001ce	0·84 ± 0·01a	4·10 ± 0·05b	47·84 ± 0·51e	5·03 ± 0·09Ba	0·45 ± 0·02C	0·16 ± 0·01C
	Middle	106·01 ± 21b	54·76 ± 4·58bcd	2·76 ± 0·10ab	0·051 ± 0·002ab	0·90 ± 0·02bc	3·85 ± 0·07ab	54·44 ± 0·98cd	4·43 ± 0·10Bb	0·55 ± 0·04B	0·2 ± 0·01B
	Inner	106·73 ± 21·18b	48·79 ± 4·46ac	2·92 ± 0·17ab	0·052 ± 0·004abc	0·92 ± 0·03b	3·92 ± 0·13ab	58·27 ± 1·49a	4·32 ± 0·12Bc	0·61 ± 0·06A	0·22 ± 0·02A
S	Outer	169·14 ± 27·06a	62·69 ± 4·47d	2·71 ± 0·04ab	0·055 ± 0·001bcd	0·85 ± 0·01ac	4·06 ± 0·05b	52·08 ± 0·86d	4·92 ± 0·09Ba	0·41 ± 0·02C	0·15 ± 0·01C
	Middle	197·21 ± 21·07ad	55·36 ± 4·67bcd	2·68 ± 0·08ab	0·048 ± 0·001ad	0·88 ± 0·02ab	3·84 ± 0·06ab	56·96 ± 0·98bc	4·53 ± 0·12Bb	0·51 ± 0·03B	0·19 ± 0·01B
	Inner	174·69 ± 14·06ab	57·71 ± 3·94bcd	2·85 ± 0·12ab	0·049 ± 0·002ab	0·92 ± 0·03b	3·91 ± 0·10ab	59·32 ± 1·27ab	4·32 ± 0·13Bc	0·57 ± 0·04A	0·21 ± 0·02A
W	Outer	96·86 ± 28·81ab	57·99 ± 3·88cd	2·59 ± 0·05b	0·055 ± 0·001be	0·83 ± 0·01a	3·93 ± 0·05bc	47·54 ± 0·72e	4·84 ± 0·08ABa	0·44 ± 0·02C	0·17 ± 0·01C
	Middle	262·51 ± 24·04cd	60·06 ± 3·1cd	2·92 ± 0·08a	0·055 ± 0·002bde	0·92 ± 0·02b	4·02 ± 0·07bc	55·12 ± 1·04c	4·52 ± 0·12ABb	0·49 ± 0·04B	0·17 ± 0·01B
	Inner	274·75 ± 21·78c	45·91 ± 4·33ab	2·77 ± 0·12ab	0·048 ± 0·002ab	0·94 ± 0·03b	3·73 ± 0·12ac	58·82 ± 1·46ac	4·08 ± 0·15ABc	0·62 ± 0·05A	0·22 ± 0·01A

Upper and lower case letters indicate an absence of interaction between factors.
L_{azi} and L_{tilt}, $n = 1394$; L_{area}, $n = 1252$; SLA and LDM, $n = 1247$; L_{width}, L_{length} and L_{index}, $n = 1219$; SAL_d, $n = 1252$; $STAR_d$, $n = 1394$.
Levels with different letters indicate significant differences ($\alpha < 0{\cdot}05$).

Potential leaf exposure across the tree crown over time

The integrated values of SAL_d and $STAR_d$ (product of the interaction of leaf angles and the sun's trajectory during the chosen day) were only significant among crown layers (Table 2). Leaves of the inner layer had greater SAL_d and $STAR_d$ values than leaves in the middle and outer layers (Table 3), thus experiencing a smaller potential reduction in the intercepting surface due to the sun's trajectory and leaf angles. On average, leaves in the inner layer exposed a surface area of 0·14 cm^2 and had 4 % higher $STAR_d$ than the outer layer during the chosen day. Values of SAL_t and $STAR_t$ showed a significant effect of the triple interaction among crown sector, layer and day period (Table 4). Leaves in each sector and layer were distinctly exposed to direct radiation during the selected periods. The outer layer of the crown had sustained adaxial exposure from T1 to T4. However, SAL_t values remained $<2\,cm^2$ in all crown sectors and reached their maximum between T2 and T3 (mid-morning and midday; Fig. 2A, dashed lines with squares). Therefore, leaves in the outer layer experienced a sustained reduction of the exposed surfaces during the day. On the contrary, middle and inner layers displayed distinct SAL_t patterns across crown sectors over the course of the day, achieving full interception and hence experiencing a lower reduction than the outer layer (Fig. 2A, dotted lines with triangles, and solid lines with circles). In the N sector, the inner and middle layers had similar daily SAL_t patterns to the outer layer. The remaining sectors had greater SAL_t values ($>2\,cm^2$) and variance during the day. Leaves in the middle and inner layers in the E, S and W sectors reached maximum SAL_t in consecutive periods during the day from T2 to T4, enabling spatio-temporal complementarity (Fig. 2A, left to right). The variation in SAL_t pattern over the selected periods increased from the outer layer to the middle and inner layers of the crown across crown sectors, except for the N sector (Fig. 2A). Likewise, as leaf area did not differ among crown positions, the $STAR_t$ patterns were similar to SAL_t (Fig. 2B). Maximum $STAR_t$ values reached 0·6 in the outer layer, whereas middle and inner layers had a maximum $STAR_t$ of 0·8 (except in the N sector; Fig. 2B).

Crown layers and sectors as a function of leaf angles (L_{azi} and L_{tilt}) had similar $STAR_d$ values over time (integrated values from sunrise to sunset). Average leaf angles for each crown sector and layer for $STAR_d$ differed by around 5–6 % between the inner and outer layers during the day. However, the sun's trajectory from east to west determines that all leaves oriented in these directions (L_{azi} ~90° or 270°) will experience the greatest variance in the exposed surface during the day—specifically, if they display high L_{tilt} angles, as shown by the outer layer (except the S sector), the inner and middle layers of the E sector (all with north-east to south-east orientations) and the inner and middle layers of the W sector (oriented to the west). These positions in the crown maximize potential light interception (the angle of incidence of the sunbeam is perpendicular to the plane of the leaf) either in the morning or the afternoon periods due to the displayed L_{azi}. In spite of a small variation in $STAR_d$ values in the different crown positions during the day, leaves in the middle and inner layers of the N sector and in all layers of the S sector experienced a greater reduction in the maximum surface to intercept light ($STAR_d < 1$) and less variability over time.

TABLE 4. *Summary statistics for the best linear mixed model fitted to the instantaneous SAL_t and $STAR_t$ displayed within the crown with the fixed effects of crown sector (N, S, E, W), crown layer (outer, middle and inner), day period (T1–T5) and interactions between crown sector and crown layer, day period and crown sector, day period and crown layer, and the triple interaction*

	SAL_t				$STAR_t$		
	numDF	denDF	*F*-value	*P*-value	denDF	*F*-value	*P*-value
(Intercept)	1	6192	105·20	**<0·0001**	6901	322·43	**<0·0001**
Sector	3	6192	1·85	0·14	6901	1·08	0·35
Layer	2	6192	13·86	**<0·0001**	6901	13·11	**<0·0001**
Day period	4	6192	284·64	**<0·0001**	6901	323·00	**<0·0001**
Sector × day period	12	6192	42·58	**<0·0001**	6901	39·50	**<0·0001**
Sector × layer	6	6192	0·55	0·77	6901	1·44	0·20
Layer × day period	8	6192	12·44	**<0·0001**	6901	10·68	**<0·0001**
Sector × layer × day period	24	6192	17·94	**<0·0001**	6901	14·73	**<0·0001**

numDF, numerator degrees of freedom; denDF, denominator degrees of freedom.
The standard deviation of the random component (biovolume) was 0·20 and 0·04 for the model fitted to SAL_d and $STAR_d$, respectively.
Statistically significant values are indicated in bold text.

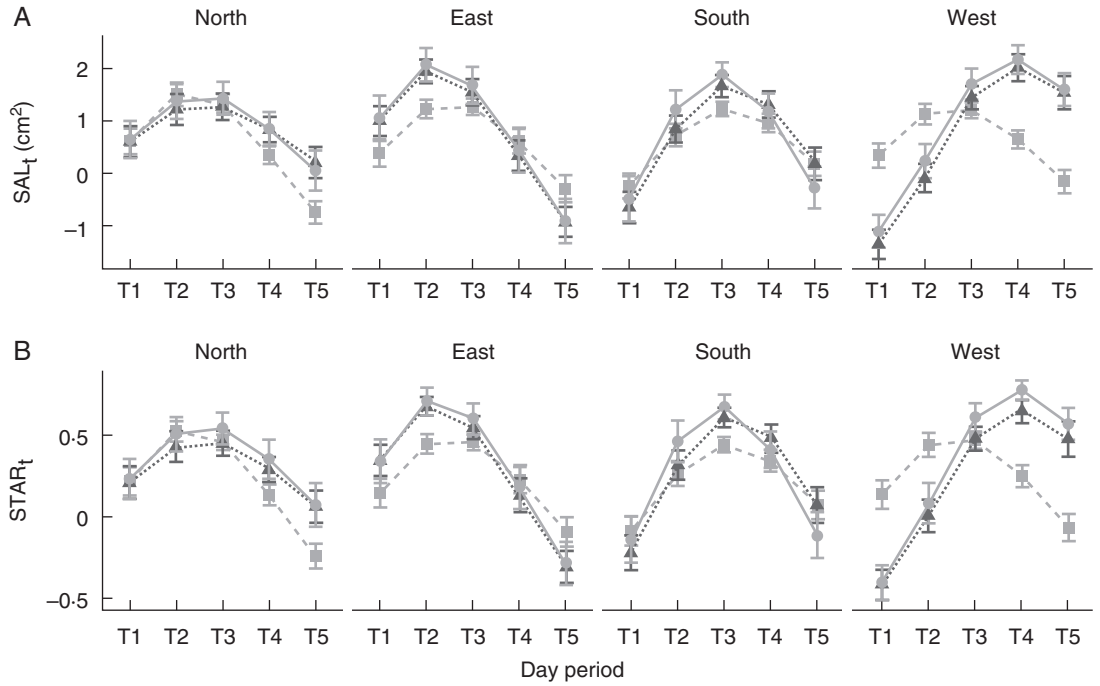

Fig. 2. Interaction plot of the best-fit model for SAL_t (A) and $STAR_t$ (B) among crown sectors (columns) and crown layers (squares and dashed lines, outer; triangles and dotted lines, middle; circles and solid lines, inner) over the simulated day periods (T1–T5). Symbols show adjusted means ± 2 s.e. Negative SAL_t and $STAR_t$ values indicate abaxial interception. Models: [SAL ∼ crown sector × crown layer × day period + (1|biovolume)] $n = 6260$; [STAR ∼ crown sector × crown layer × day period + (1|biovolume)], $n = 6970$.

DISCUSSION

The results showed a high variance in leaf traits within the tree crown. The apparent non-random distribution of leaf angles across crown positions resulted in complementary patterns of potential leaf exposure to direct radiation during the day among crown sectors and layers. Although leaf angles differed among crown positions, the potential exposed leaf area was similar among sectors, with small differences between crown layers during the day. However, displayed leaf angles determined distinct temporal patterns of leaf exposure in contrasting day periods. Leaves in the outer layer had the greatest reduction in exposed surface compared with leaves in the inner and middle layers (specifically around midday). Leaf exposure was sustained during the day, with maxima skewed towards morning periods. On the contrary, leaves in the middle and inner layers achieved greater interception and high variance among day periods depending on the crown sector. These findings suggest that leaf phenotypes are adjusted in a particular manner across the spatial volume of the crown and that the leaf's potential exposure depends on the location of the leaf within the tree crown. Moreover, differential leaf trait expression across the crown has shown a significant correlation with light interception patterns, carbon assimilation and export between contrasting light conditions within the crown (Granado-Yela *et al.*, 2011).

To our knowledge, the present study is the first to report such non-random distribution of leaf orientation and inclination angles

in trees. The observed angles are congruent with phenotypic integration of potential exposed surfaces across the canopy. The effects of non-random leaf orientation and inclination angles in high-irradiance environments have been shown to enhance water-use efficiency at high solar angles and to provide equivalent or higher carbon gain compared with other possible orientations (Jurik *et al*., 1990; James and Bell *et al*., 2000) and even linked to reproduction (Werk and Ehleringer, 1986). The environmental heterogeneity across the tree crown of isolated trees depends on exogenous conditions but also on modification of the within-canopy environment caused by the crown architecture. As a consequence, crown performance depends not only on the environment in which the tree grows but, to a large extent, on the modification of the environment caused by tree crown growth and its architecture (Rubio de Casas *et al*., 2007, 2011).

Differences in leaf inclination and orientation angles across tree crown positions can yield complex patterns of light interception and lead to a complementary strategy of leaf exposure to direct radiation during the day. Despite the fact that our measurements neither considered self-shading from adjacent layers and other phytoelements nor the diffuse portion of the radiation, the inner and middle layer had near-optimal leaf inclination angles to maximize light interception in the studied location (L_{tilt} ~40°; Mehleri *et al*., 2010). Moreover, L_{azi} varied, matching on average the crown sector in which the leaf was located. This configuration enabled a consecutive achievement of maximum interception during the day by each crown sector and a potentially constant assimilation even during high-irradiance periods, such as around midday. On the contrary, the outer layer of leaves experienced less variation during the day in the light interception patterns, due to high L_{tilt} values and L_{azi} with eastern and south-eastern orientations. Such relative spatial positions can enable sustained carbon assimilation throughout the day despite the diurnal variation in solar light intensity and angle of incidence (Granado-Yela *et al*., 2011). Our results showed that leaves in the outer layer potentially experience a decrease that is 5–6 % greater in the exposed leaf area than in the inner layer during the day, due to the cosine law, and that they do not achieve full exposure at any given time. Accordingly, the outer layer of leaves had lower SLA values than the inner and middle layers. Optimization theories suggest that the investment in SLA across crown positions should be inversely proportional to the intercepted light (Field, 1983; Farquhar, 1989). The observed configuration of the outer layer of the crown (more vertical leaves, low SLA, high L_{index}, low SAL_d and $STAR_d$) suggests a trade-off between maximizing interception and avoiding excessive radiation loads during high-irradiance periods (midday, summer).

Minimizing the negative impact of photoinhibition by displaying vertical leaf angles (structural photoprotection) can compensate for low daily carbon gains and may enable interception of non-saturating photon flux density in high-irradiance environments (Ehleringer and Werk, 1986; Valladares and Pugnaire, 1999; Werner *et al*., 2001; Falster and Westoby, 2003). This strategy should be similar across crown sectors. However, according to our measurements the outer layer in the S sector (expected to endure higher irradiance and heat loads in the northern hemisphere) had greater interception area during T3 than in any other day period. An explanation for this paradoxical finding (i.e. maximizing light interception during the central hours of the day, yet being less exposed than other sectors) may rely upon structural photoprotection. This sector displayed L_{azi} values oriented towards south-eastern aspects. Facing south with high leaf inclination angles may contribute to the avoidance of dynamic photoinhibition by ensuring that full leaf exposure is not reached at any given time. However, avoidance of direct sunlight by the outer leaves in the S sector during T3 would result in long-lasting, high-intensity irradiance pulses reaching the inner and middle layers. Such pulses may be at least as harmful for the middle and inner layers as they are for the outer layer. Consequently, inner and middle layers in the S sector had similar L_{tilt} angles to the outer layer. This is congruent with previous findings of minimal photoinhibition during midday and subsequent recovery of assimilation in the afternoon (Granado-Yela *et al*., 2011). Factors that increase self-shading constitute crucial attributes of plant survival in high-irradiance environments despite their ability to adjust physiologically to stress (Valladares and Pearcy, 1997; Howell *et al*., 2002; Pearcy *et al*., 2005). If the outer layer allows a higher fraction of the radiation to penetrate into deeper layers, the use of light and whole-crown photosynthesis might be more efficient (Watson and Witts, 1959; Verhagen *et al*., 1963; Terashima and Hikosaka, 1995). Nevertheless, until self-shading and the whole portion of the radiation, i.e. direct and diffuse light, are taken into consideration, the optimization of the light interception strategy through the expression of multiple leaf syndromes at the crown scale will remain a working hypothesis. Even so, we believe that our work provides substantial evidence of a distinct expression of leaf phenotypes across the tree crown that encourages further research to assess the light environment within crowns and the implications in terms of light use efficiency at the individual scale.

The expression of leaf traits within isolated trees of *O. europaea* varies continuously through the crown in a gradient of leaf morphotypes and leaf angles depending on the exposure and location of individual leaves. The apparent non-random distribution of leaf angles across the tree crown yields complementary patterns of potential exposure of the leaves among crown positions through a single day. The distinct expression of leaf traits within trees suggests spatio-temporal integration of the leaves across the tree crown. Indeed, plants adapt morphologically and physiologically to subtle environmental differences at smaller scales than the individual level (de Kroon *et al*., 2005; Esteso-Martínez *et al*., 2006), which could result in interactions between functionally differentiated subunits and potentially in an increase in performance at the organism level (de Kroon *et al*., 2005; Granado-Yela *et al*., 2011). However, tree crowns are complex multifunctional structures that might be subjected to several pressures and constraints (Pearcy *et al*., 2005). A deeper understanding of the function of the tree crown requires additional research to characterize the local environment within the tree crown and to determine the evolutionary and ecological implications of the spatial variation of leaf traits within individuals.

SUPPLEMENTARY DATA

Supplementary data are available online at www.aob.oxfordjournals.org and consist of the following. Tables S1–S10: Details of linear mixed models of leaf traits. Summary statistics for the best linear mixed model fitted to leaf traits, the fixed effects of crown sector and crown layer, the interactions between them and biovolume as a random effect. Figure S1: Histograms

with means of leaf tilt (A) and leaf azimuth (B) for each crown sector and layer binned every 5° and 10°, respectively.

ACKNOWLEDGEMENTS

We wish to thank M. D. Jiménez, A. López-Pintor, A. Vázquez and K. Carrillo for their expertise and help during study design and field sampling, and H. Huber, H. During, T. DeJong and two anonymous referees for their contributions at the final stage. This research was supported by the Spanish Ministry of Science and Education (CGL2009-10392) and through an FPI grant to A.G.E. (BES-2010-032767). We are also indebted to the Madrid Regional Government (REMEDINAL-2, S2009/AMB-1783).

LITERATURE CITED

Ackerly DD, Bazzaz FA. 1995. Seedling crown orientation and interception of diffuse radiation in tropical forest gaps. *Ecology* **76**: 1134–1146.

Bouvet JM, Vigneron P, Saya A. 2005. Phenotypic plasticity of growth trajectory and ontogenic allometry in response to density for *Eucalyptus* hybrid clones and families. *Annals of Botany* **96**: 811–821.

Bretz F, Hothorn T, Westfall P. 2004. *Multcomp: multiple tests and simultaneous confidence intervals*. R Package, Version 0.4-8. http://ftp.auckland.ac.nz/software/CRAN/src/contrib/Descriptions/multcomp.html (last accessed 8 February 2016).

Carter GA, Smith WK. 1985. Influence of shoot structure on light interception and photosynthesis in conifers. *Plant Physiology* **79**: 1038–1043.

Cavender-Bares J, Kitajima K, Bazzaz FA. 2004. Multiple trait associations in relation to habitat differentiation among 17 Floridian oak species. *Ecological Monographs* **74**: 635–662.

de Kroon H, Huber H, Stuefer JF, van Groenendael JM. 2005. A modular concept of phenotypic plasticity in plants. *New Phytologist* **166**: 73–82.

Ehleringer JR, Werk KS. 1986. Modifications of solar radiation absorption patterns and implications for carbon gain at the leaf level. In: T Givnish, ed. *On the economy of plant form and function*. Cambridge: Cambridge University Press, 57–82.

Escribano-Rocafort AG, Ventre-Lespiaucq AB, Granado-Yela C, *et al.* 2014. Simplifying data acquisition in plant canopies; measurements of leaf angles with a cell-phone. *Methods in Ecology and Evolution* **5**: 134–140.

Esteso-Martínez J, Valladares F, Camarero, JJ, Gil-Pelegrín E. 2006. Crown architecture and leaf habit are associated with intrinsically different light-harvesting efficiencies in *Quercus* seedlings from contrasting environments. *Annals of Forest Science* **63**: 511–518.

Falster DS, Westoby M. 2003. Leaf size and angle vary widely across species: what consequences for light interception? *New Phytologist* **158**: 509–525.

Falster DS, Brännström A, Dieckmann U, Westoby M. 2011. Influence of four major plant traits on average height, leaf-area cover, net primary productivity, and biomass density in single-species forests: a theoretical investigation. *Journal of Ecology* **99**: 148–164.

Farnsworth KD, Niklas, KJ. 1995. Theories of optimization, form and function in branching architecture in plants. *Functional Ecology* **9**: 355–363.

Farque L, Sinoquet H, Colin F. 2001. Canopy structure and light interception in *Quercus petraea* seedlings in relation to light regime and plant density. *Tree Physiology* **21**: 1257–1267.

Farquhar GD. 1989. Models of integrated photosynthesis of cells and leaves. *Philosophical Transactions of the Royal Society of London B: Biological Sciences* **323**(1216): 357–367.

Field C. 1983. Allocating leaf nitrogen for the maximization of carbon gain: leaf age as a control on the allocation program. *Oecologia* **56**: 341–347.

Garnier E, Laurent G, Bellmann A, *et al.* 2001. Consistency of species ranking based on functional leaf traits. *New Phytologist* **152**: 69–83.

Granado-Yela C, García-Verdugo C, Carrillo K, Rubio de Casas R, Kleczkowski LA, Balaguer L. 2011. Temporal matching among diurnal photosynthetic patterns within the crown of the evergreen sclerophyll *Olea europaea* L. *Plant, Cell & Environment* **34**: 800–810.

Gratani L, Covone F, Larcher W. 2006. Leaf plasticity in response to light of three evergreen species of the Mediterranean maquis. *Trees* **20**: 549–558

Howell CJ, Kelly D, Turnbull MH. 2002. Moa ghosts exorcised? New Zealand's divaricate shrubs avoid photoinhibition. *Functional Ecology* **16**: 232–240.

James SA, Bell DT. 2000. Leaf orientation, light interception and stomatal conductance of *Eucalyptus globulus* ssp. *globulus* leaves. *Tree Physiology* **20**: 815–823.

Jurik TW, Chabot JF and Chabot BF. 1979. Ontogeny of photosynthetic performance in *Fragaria virginiana* under changing light regimes. *Plant Physiology* **63**: 542–547.

Jurik TW, Zhang H, Pleasants JM. 1990. Ecophysiological consequences of non-random leaf orientation in the prairie compass plant, *Silphium laciniatum*. *Oecologia* **82**: 180–186.

Marks CO, Lechowicz MJ. 2006. Alternative design and the evolution of functional diversity. *American Naturalist* **167**: 55–66.

Mehleri ED, Zervas PL, Sarimveis H, Palyvos JA, Markatos NC. 2010. Determination of the optimal tilt angle and orientation for solar photovoltaic arrays. *Renewable Energy* **35**: 2468–2475.

Moorcroft PR, Hurtt GC, Pacala SW. 2001. A method for scaling vegetation dynamics: the ecosystem demography model (ED). *Ecological Monographs* **71**: 557–586.

Oker-Blom P, Smolander H. 1988. The ratio of shoot silhouette area to total needle area in Scots pine. *Forest Science* **34**: 894–906

Pearcy RW, Yang W. 1996. A three-dimensional crown architecture model for assessment of light capture and carbon gain by understory plants. *Oecologia* **108**: 1–12.

Pearcy, RW, Muraoka H, Valladares F. 2005. Crown architecture in sun and shade environments, assessing function and trade-offs with a three-dimensional simulation model. *New Phytologist* **166**: 791–800.

Planchais I, Sinoquet H. 1998. Foliage determinants of light interception in sunny and shaded branches of *Fagus sylvatica* (L.). *Agricultural and Forest Meteorology* **89**: 241–253.

R Development Core Team. 2008. R: A language and environment for statistical computing. R Foundation for Statistical Computing, Vienna, Austria. http://www.R-project.org (last accessed 8 February 2016).

Rubio de Casas R, Vargas P, Perez-Corona E, *et al.* 2007. Field patterns of leaf plasticity in adults of the long-lived evergreen *Quercus coccifera*. *Annals of Botany* **100**: 325–334.

Rubio de Casas R, Vargas P, Pérez-Corona E, Manrique E, García-Verdugo C, Balaguer L. 2011. Sun and shade leaves of *Olea europaea* respond differently to plant size, light availability and genetic variation. *Functional Ecology* **25**: 802–812.

Sack L, Melcher PJ, Liu WH, Middleton E, Pardee T. 2006. How strong is intracanopy leaf plasticity in temperate deciduous trees? *American Journal of Botany* **93**: 829–839.

Sarlikioti V, de Visser PHB, Buck-Sorlin GH, Marcelis LFM. 2011. How plant architecture affects light absorption and photosynthesis in tomato: towards an ideotype for plant architecture using a functional–structural plant model. *Annals of Botany* **108**: 1065–1063.

Terashima I, Hikosaka K. 1995. Comparative ecophysiology of leaf and canopy photosynthesis. *Plant, Cell & Environment* **18**: 1111–1128.

Uemura A, Harayama H, Koike N, Ishida A. 2006. Coordination of crown structure, leaf plasticity and carbon gain within the crowns of three winter-deciduous mature trees. *Tree Physiology* **26**: 633–641.

Valladares F, Niinemets U. 2008. Shade tolerance, a key plant feature of complex nature and consequences. *Annual Review of Ecology Evolution and Systematics* **39:** 237–257.

Valladares F, Pearcy RW. 1997. The functional ecology of shoot architecture in sun and shade plants of *Heteromeles arbutifolia* M. Roem., a Californian chaparral shrub. *Oecologia* **114**: 1–10.

Valladares F, Pugnaire FI. 1999. Tradeoffs between irradiance capture and avoidance in semi-arid environments assessed with a crown architecture model. *Annals of Botany* **83**: 459–469.

Valladares F, Dobarro I, Sánchez-Gómez D, Pearcy RW. 2005. Photoinhibition and drought in Mediterranean woody saplings: scaling effects and interactions in sun and shade phenotypes. *Journal of Experimental Botany* **56**: 483–494.

Verhagen AMW, Wilson JH, Britten EJ. 1963. Plant production in relation to foliage illumination. *Annals of Botany* **27**: 627–640.

Watson DJ, Witts KJ. 1959. The net assimilation rates of wild and cultivated beets. *Annals of Botany* **23**: 431–439.

Werk KS, Ehleringer J. 1986. Effect of nonrandom leaf orientation on reproduction in *Lactuca serriola* L. *Evolution* **40**: 1334–1337.

Werner C, Ryel RJ, Correia O, Beyschlag W. 2001. Structural and functional variability within the canopy and its relevance for carbon gain and stress avoidance. *Acta Oecologica* **22**: 129–138.

Werner C, Correia O, Beyschlag W. 2002. Characteristic patterns of chronic and dynamic photoinhibition of different functional groups in a Mediterranean ecosystem. *Functional Plant Biology* **29**: 999–1011.

Wilson AJ, Nussey DH. 2010. What is individual quality? An evolutionary perspective. *Trends in Ecology & Evolution* **25**: 207–214.

APPENDIX

Abbreviations

L_{area}, area of one side of leaf (cm^2).
L_{width}, leaf lamina maximum width (cm).
L_{length}, leaf maximum length (cm).
LDM, leaf dry mass (g).
SLA, specific leaf area ($cm^2\,g^{-1}$).
L_{index}, leaf length-to-width ratio. Dimensionless; higher values indicate elongated leaves.
L_{tilt}, leaf lamina inclination angle (°). 90°, vertical inclination, 0°, leaves lie horizontal.
L_{azi}, Leaf lamina azimuth angle (°). Deviation angle from true north of the projection of a normal vector to the leaf's lamina surface.
SAL, silhouette area of the leaf blade (cm^2). Negative values indicate underside exposure.
STAR, silhouette area of the leaf blade-to-area ratio. Dimensionless; negative values indicate underside exposure.
SAL_t, silhouette area of the leaf blade during chosen periods (T1–T5, cm^2).
$STAR_t$, silhouette area of the leaf blade-to-area ratio during chosen periods (T1–T5). Dimensionless, 0–1.
SAL_d, silhouette area of the leaf blade integrated over a day period (cm^2).
$STAR_d$, silhouette area of the leaf blade-to-area ratio integrated over a day period. Dimensionless.
T1 – T5, day period. Equivalent periods were chosen at each location from midday (T3, maximum sun's elevation angle) towards sunrise (T1) and sunset (T5).
AF, Aldea del Fresno population.
SL, San Luis population.